Machining and Heat Treatment Effects on the Fatigue Properties of Maraging Steel Produced by DMLS

S. Ćirić-Kostić[1], N. Bogojević[1], A. Vranić[1*], D. Croccolo[2], M. De Agostinis[2], S. Fini[2], G. Olmi[2]
[1]Faculty of Mechanical and Civil Engineering in Kraljevo, University of Kragujevac, Serbia
[2]Department of Industrial Engineering (DIN), University of Bologna, Bologna, Italy

DMLS enables manufacturing of functional parts with complex shapes in a short time. This technology has some drawbacks: high manufacturing cost, residual stresses, and volume and surface imperfections. These problems can be solved by additional post processing (machining, heat treatment and shot peening), which increase manufacturing cost and time. There is an increasing interest towards the mechanical response of parts in the as-fabricated state. Being able to manage these parts, without the need for machining or heat treatment, would strongly increase the great potentials of this technology. The present study deals with the effect of machining and heat treatment (aging at the temperature of 490°C for 6 hours) on the fatigue response of DMLS Maraging steel parts, with vertical build orientation. Specimens have been manufactured according to ISO 1143 for fatigue tests under rotating four-point bending. The experimental campaign has been arranged as a 2-by-2 factorial plane, with a total amount of four treatment combinations. The first results, processed also by tools of analysis of variance, indicate that heat treatment has the greatest beneficial impact on the fatigue response and that even without machining a fatigue limit in the order of 25% of the ultimate tensile strength can be achieved.

Keywords: Fatigue strength, Maraging steel, Additive manufacturing, Direct Metal Laser Sintering, Aging heat treatment, Machining.

1. INTRODUCTION

Additive Manufacturing (AM) process is based on layer manufacturing, without any additional tools or machining processes [1-4]. Direct Metal Laser Sintering (DMLS) and Selective Laser Melting are the two most important Additive Manufacturing technologies. Both of them are powder bed-based technologies.

Concept of layered built parts dates from more than one century. AM enables manufacturing without tools, using just one AM machine fed by a CAD model. CAD model is split into two-dimensional layers with constant thickness, by specific software. These layers cabn be regarded as areas that will be melted with thickness corresponding to the distance between layers (thickness of the layer). Every new layer is fused with the previous one during the AM process. Part is built, by repeating this process until the last layer is stacked.

There are several AM technologies that are divided, based on the type of material, how material is applied, fused etc. Powder Bed technology is based on material application on the entire building surface; afterwards, the laser or electron beam melts the area that corresponds to the sliced surface. The process is repeated, until part completion. Wire or powder feed technology is based on step-by-step material application and melting, forming the surface that correspond to the sliced layer. In this case, material is applied just to the surface that is being manufactured. A further classification of the AM techniques could be made, based on the principle of material melting (laser beam, electro beam, electro-arc etc.). In almost all the technologies for AM of metal parts, the material is completely melted and bonding between layers is achieved during solidification. DMLS and SLM are nowadays quite close technologies. Their different names mostly arise from different trademarks [5]. At the early stages of development of these technologies, components after manufacturing were porous, density was not full due to partial fusion. The sintering process was different and material was based on Iron, Copper and Nickel alloy. Additional processing was needed to achieve better density and fusion [6,7].

AM technologies are used not only in industrial applications but also in the medical field. It is possible to use these technologies and material, to build custom implants. Using 3D CT scanners, it is possible to model implants that perfectly fit the person's need [8-10]. These materials have good bio-compatibility that gives them good potential for dental and medical purposes [11].

Since AM of metal parts is based on manufacturing of fully functional parts that can be built directly into machine, with minimal post processing, mechanical and physical characteristics of the built parts are of high importance. Layer based manufacturing provides characteristic microstructure of the build parts that is different than casted structure of the same material. In AM, material melting takes place on one plane (build plane), whereas the stacking direction is normal to this plane. Material melting and cooling rates are very high. Fast melting is the result of high energy concentration. Fast cooling arises from the small amount of melted material with low surrounding temperature. This high temperature gradient usually induces high residual stresses. Part building starts on thick steel plate (base-plate). Part can be built directly on the plate or with a support structure, generated between plate and part. Its purpose is part constraining, moreover it facilitates heat flow from the part during the scanning (melting) process. Support structure needs to be strong enough, to restrain any kind of deformation that residual stress can cause.

With casting technology, a much larger amount of material keeps heat accumulated for a longer period time. Melting and solidification of material is a slow process

*Corresponding author: Faculty of the Mechanical and Civil Engineering, 36000 Kraljevo, Dositejeva 19, vranic.a@mfkv.kg.ac.rs

and involves the whole volume. For this reason, it is interesting to explore influence of layer manufactured structure on mechanical properties. Machine manufactures usually provide some data regarding the mechanical properties of AM built parts in the material datasheets [12]. However, these mainly deal with static properties, such as ultimate tensile strength, yield strength, hardness, mechanical characteristics after ageing etc.

Maraging steel is one of the most promising materials, for use in Additive Manufacturing [13]. Density of AM built parts are >90%. Hardness of AM built parts from maraging steel is similar to those made by conventional ways like casting. It has good mechanical characteristics and it can be a good candidate for high-carbon steel substitution. It is resistant to corrosion and crack initiation during tempering and it has good machinability [14-16]. It has a relatively high ultimate tensile strength (*UTS*) after the heat treatment, around 2000MPa. Thanks to its high *UTS*, it is a promising material to be used for complex structures exposed to high states of load. This becomes more attractive, considering that AM technologies gives the chance to build multi-part object as a single part [17]. Research contributions on the Fatigue limit (*FL*) and the fatigue strength (*FS*) of Maraging steel made by some of AM processes are quite limited, to the authors' best knowledge. This paper presents a follow-up of a previous research by the same authors [18].

Components produced by AM can have different orientation with respect to the stacking direction of the layers. The aim of the previous research was to explore the effect of build orientation on the fatigue strength of Maraging Steel samples built by DMLS EOS M280 machine. The obtained results indicate that part orientation did not have significant effect on *FS* and *FL*.

Literature studies dealing with orientation influence on the mechanical properties of the parts made by AM are few. Most of the research deals with the influence of orientation and additional post-processing on tensile strength [19-21]. Few papers are concerned with research on the part orientation effect on fatigue strength of Aluminium alloy [22-25], Inconel alloy [26] and Titanium alloy samples [27]. Review papers have been written, trying to collect all the technologies and all the available mechanical testing results [28]. However, a lack of consistency between the testing procedures and the obtained results can be noticed, when all these data are rounded together. Different technologies provide different results for same materials. This may be due to the lack of Standards in AM that define the parameters of the process, how building preparation of samples should be managed, etc.

There is an increasing interest in lowering down post-manufacturing expenses in AM, and in speeding up the process from design to installation. Sometimes, post processing is not possible, for instance, when treating lattice structures, cooling channels in injection moulds or in turbine blades. In particular, machining or shot-peening cannot be performed on internal surfaces. This was the main motivation that led to this study. This topic has been tackled experimentally: for this purpose, an experimental campaign has been arranged as a 2-by-2 factorial plane, with a total amount of four treatment combinations as shown in Table 1, presenting four sample types, one for each of the treatment combinations.

Table 1: 2-by-2 research plan

N Not heat treated As Built	**M** Not heat treated Machined with 0.5mm allowance
H Heat treated As Built	**1** Heat treated Machined with 0.5mm allowance

As an extension of the previous research [18], this paper focuses on the effects of heat treatment and machining influence on *FS* and *FL*. Samples without machining, named "as built" underwent only shot peening as surface post processing.

2. MATERIALS AND METHODS

Testing procedure was based on ISO 1143 Standard for rotating bending fatigue testing [29]. Standard defines testing procedure, loads and specimen geometry. Specimens were designed with cylindrical smooth geometry with reduction at the gage cross section. Specimen geometry with uniform 6mm diameter at the gage the as smallest dimension purposed by the Standard, has been chosen as the best compromise, considering the high manufacturing costs. A drawing of the specimen is shown in Fig. 1. The specification regarding surface quality was not considered for the "as built" to properly account for the influence of machining.

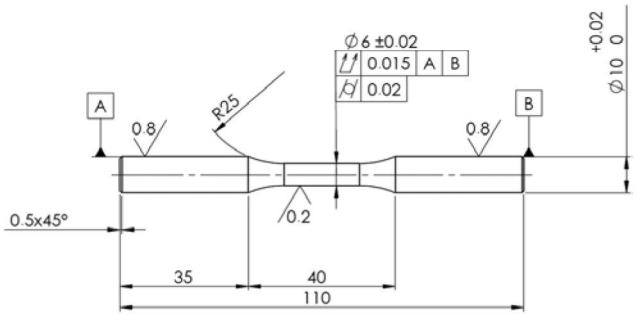

Figure 1: Specimen drawing with the 6mm diameter at gauge, according the ISO 1143 standard

The specimens have been manufactured by M280 DMLS machine (EOS GmbH – Electro Optical Systems, Germany), equipped by Ytterbium fibre laser with 200W power and emitting 0.2032mm thickness and 1064nm wavelength infrared light beam [30]. Specimen material was MS1 maraging steel (EOS GmbH – Electro Optical Systems, Germany), equivalent to 1.2709 steel [31]. Chemical composition of the material is provided in Table 2. Specimen manufacturing was done in the processing chamber of the machine. The recoater applies material from the dispenser platform on building plate and takes excess material onto collector platform. Building starts on the base plate with working area of 250×250mm in horizontal plane and with maximum building height up to 325mm. Base plate was preheated to the temperature of 40°C.

Table 2: Chemical composition of MS1 Maraging Steel by EOS

	Fe	Ni	Co	Mo	Ti	Al	Cr	Cu	C	Mn	Si	P	S
%		17-19	8.5-9.5	4.5-5.2	0.6-0.8	0.05-0.15	≤0.5	≤0.5	≤0.03	≤0.1	≤0.1	≤0.01	≤0.01

Manufacturing process typically takes place in nitrogen inert atmosphere, generated from compressed air by nitrogen generator that is built inside machine. Process chamber consists of three platforms and recoater: The Dispenser platform, where material powder is contained, the Building platform, on which the base plate is set and building process is done, the Collector platform for the collection of excess material. Schematics of the building chamber is presented on Fig. 2

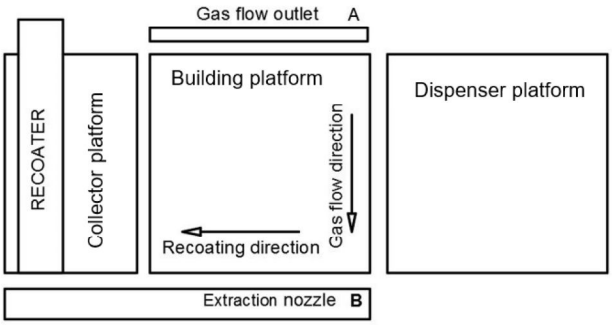

Figure 2. Process chamber schematics

Material is applied with 40µm thickness that corresponds to layer thickness for the MS1 Maraging Steel. Building parameters (laser speed, laser power, laser offset, layer thickness etc.) of the EOSINT M280 for MS1 sample manufacturing were kept constant. They were provided by the EOS as a predetermined set of parameters named "PERFORMANCE". This parameter set is a good compromise between good surface quality and manufacturing speed, for which EOS warrants mechanical characteristics of the built parts.

Scanning strategy was set in such way, where laser scans surface in parallel traces in one layer. For next layer, scanning strategy was rotated by an angle of 67°. For every layer, the contour of the scanned surface was finally rescanned, in order to get better surface quality. Example of the scanning process is shown in Fig. 3 a).

Specimens were built directly on the base plate, without using a support structure, Fig. 3 c). Proceeding this way, the surface quality of the as built specimens could keep unaffected by the support structure teeth traces on the surface. After building process, specimens were taken from the process chamber, cleaned from excessive powder by shot-peening, using stainless steel spherical shots with 400 µm diameter. Cutting off samples from the base plate was done by wire cutting with Electrical Discharge Machining (EDM).

Samples planned for heat treatment underwent age-hardening by heating in oven. Temperature was increased from room temperature to 490 °C in 1h, afterwards, they were kept at constant temperature for additional 5h (total 6h process). This heat treatment was particularly important for lowering or relaxing the residual stresses, which arise from AM process, thus enhancing fatigue response of the built specimens [32, 33]. Since these samples were built vertically, their geometry was not influenced by residual stress. After heat treatment process, specimens were cooled to room temperature in fresh air. Shot-peening gave effect just in better surface quality and closing micro pores for as built samples. For heat treated samples surface hardening induced by plastic deformation was lost after ageing, due to relaxation of the compressive residual stresses induced by shot-peening. The effect of micro shot peening was also questionable for the machined samples, since allowance for machining was 0.5mm. There is large probability that the hardened surface following micro shot peening was removed upon machining. Finally, specimens planned for machining, underwent machining and refining by grinding with the aim of achieving the surface quality required by the ISO 1143 Standard and also to improve the fatigue performance [29].

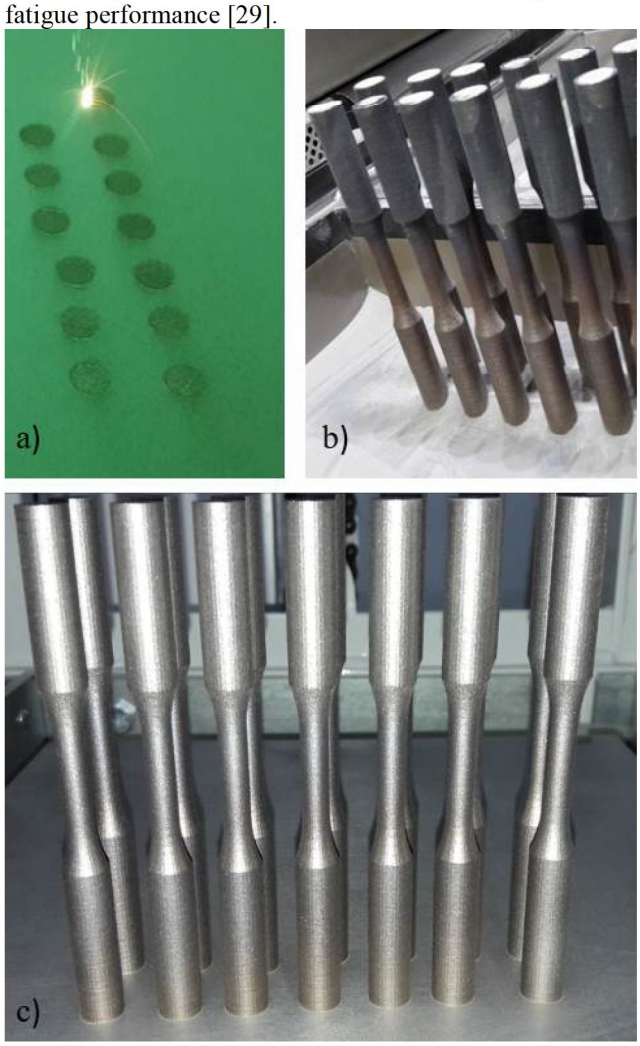

Figure 3. a) As Built specimens during scanning,

b) Specimens cleaning from powder,

c) Specimens after micro shot peening

For this research campaign, three sets of samples were built, all with vertical build orientation, with dog bone shape and shot peened. The first specimen set, type 1 (with additional age-hardening and machining with 0.5mm

allowance), was tested in the previous research campaign [18] and the related results were used here for comparisons. The second specimen set type M, for machined condition without age hardening, was built under the same conditions as the first one, with 0.5mm allowance for machining. The last two sets in the as built condition (one with age hardening, type H, the other without age hardening, type N) were built without any additional material allowance. Their surface roughness was lowered just by micro shot peening process.

Specimens were mounted on the testing rig, by tightening their heads into chuck collet, on both sides of the specimen Fig 4. Load was kept constant and bending moment was constant at gage during testing Fig. 5. The Testing rig, for four-point rotating bending was described in [18].

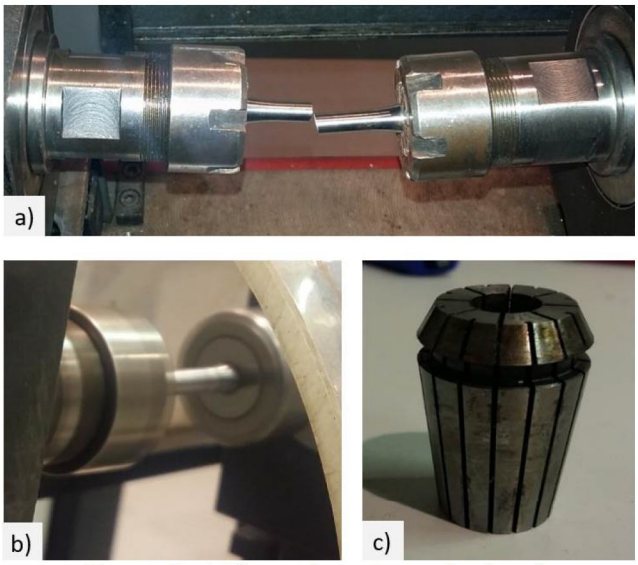

Figure 4. a) Clamped specimen after break,

b) Specimen running,

c) Chuck collet

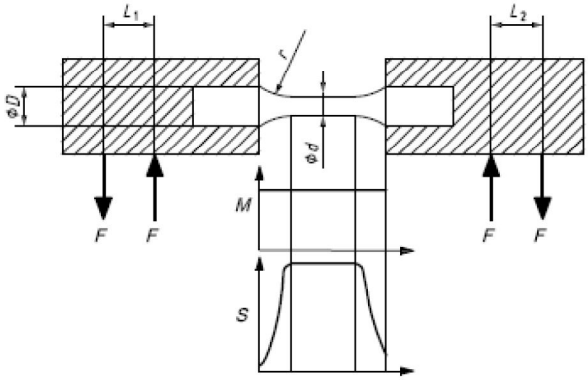

Figure 5. Load distribution

The specimens were tested until failure or until 10^7 cycles: in this case the specimen was marked as "RUN OUT". Each sample set consisted of 7 to 14 specimens. In the previous stage of the research, some samples were damaged during the manufacturing process, so they were not considered.

Using the aforementioned procedure, it was possible to obtain *FL* and the *S-N* curve for finite life domain. Fatigue limit was obtained by the Dixon stair-case method for small number of sample trials with failure or non-failure outcomes [34]. Dixon method is a modified stair-case method that makes it possible to estimate *FL* even from small series of nominal trials (in this case four to seven). Standard deviation was estimated to estimate the uncertainty and to determine the confidence band for *FL*. ISO 12107 was used for processing data in finite life domain [35]. Data were linearly interpolated in logarithmic diagram. Upper and lower limits of the logarithmic curve were determined, based on the standard deviation of fatigue life, with the probability of failure of 90% for upper limit and 10% for lower limit and with the confidence level of 90%.

3. EXPERIMENTAL

All the samples have undergone geometry measurement, to check drawing requirements accomplishment. Diameter dimension and surface roughness have been measured at the head and gauge. For this purpose, a micrometre screw gauge, (with the resolution of 0.01mm) and a portable surface roughness tester (with the resolution of 0.01 μm, Handysurf E-30A; Carl Zeiss AG, Oberkochen, Germany) have been used.

Diameter measurement checks have been done at two points at the heads, replicating measurement with 90° rotations at each point, for a total of eight replications, including both specimen heads. Diameter at the gauge was measured at three points, with two replications for each, by 90° rotation for an overall number of 6 replications.

Surface roughness on the both heads was measured at four points, with 90° angular spacing, with two replications, for a total number of eight replications per head. Surface roughness at the gauge was measured only after breakage, in same manner as at the heads, with eight replications per broken side. Specimens that survived testing, marked as run-out, were not measured for surface roughness at the gauge.

Average values of the diameter and surface roughness measurements are presented in Tables 3 to 6.

Table 3. Diameter and roughness measurement for sample type 1

	Gauge diameter			Head diameter		
Specimen ID	Mean [mm]	ST. Dev. [mm]	Roughness [μm]	Mean [mm]	ST. Dev. [mm]	Roughness [μm]
1.1	6.00	0.004	0.248	9.93	0.004	0.26
1.2	6.00	0.004	0.470	9.93	0.000	0.21
1.3	6.00	0.000	0.447	9.93	0.000	0.29
1.4	6.01	0.000	0.395	9.93	0.000	0.20
1.5	6.00	0.004	/	9.92	0.000	0.31
1.6	6.01	0.000	/	9.93	0.000	0.22
1.7	6.00	0.000	/	9.93	0.007	0.27
1.8	6.00	0.004	0.697	9.93	0.000	0.30

Specimen types 1 and M are well consistent with the drawing requirements presented in Fig.1. Measurements indicate minor diameter deviations from the drawing specifications, according to ISO 1143, for specimen types H and N. Surface roughness values for the same specimen types were almost five times higher than specifications. It is reasonable, considering that these specimens were in as-built condition. Although these specimens did not satisfy surface roughness requirements, their testing was justified by the increasing demand for as-built parts and by the need for an estimation of their

fatigue response. After measurement procedure, fatigue tests were carried out, loading the samples under four-point rotary bending.

Table 4. Diameter and roughness measurement for sample type H

	Gauge diameter			Head diameter		
Specimen ID	Mean [mm]	ST. Dev. [mm]	Roughness [µm]	Mean [mm]	ST. Dev. [mm]	Roughness [µm]
H.1	6.05	0.004	4.063	10.09	0.017	4.90
H.2	6.06	0.015	4.700	10.10	0.012	4.95
H.3	6.06	0.008	4.055	10.07	0.010	5.02
H.4	6.06	0.011	3.738	10.10	0.015	4.55
H.5	6.05	0.004	3.769	10.09	0.004	4.13
H.6	6.06	0.008	/	10.08	0.010	5.50
H.7	6.06	0.008	/	10.09	0.017	4.78
H.8	6.05	0.003	/	10.09	0.013	4.30
H.9	6.05	0.006	4.000	10.08	0.014	4.70
H.10	6.08	0.005	4.195	10.11	0.019	4.67
H.11	6.04	0.012	5.614	10.09	0.006	6.38
H.12	6.05	0.014	3.714	10.07	0.014	4.55

Table 5. Diameter and roughness measurement for sample type N

	Gauge diameter			Head diameter		
Specimen ID	Mean [mm]	ST. Dev. [mm]	Roughness [µm]	Mean [mm]	ST. Dev. [mm]	Roughness [µm]
N.1	6.08	0.012	4.24	10.07	0.020	5.54
N.2	6.09	0.010	4.12	10.08	0.004	5.48
N.3	6.08	0.008	3.97	10.06	0.010	5.19
N.4	6.09	0.008	4.37	10.07	0.013	4.74
N.5	6.09	0.005	4.57	10.07	0.019	5.28
N.6	6.09	0.009	/	10.07	0.012	4.75
N.7	6.09	0.010	/	10.08	0.007	4.43
N.8	6.08	0.007	/	10.07	0.008	4.24
N.9	6.09	0.007	4.07	10.06	0.010	4.76
N.10	6.09	0.009	5.12	10.08	0.011	5.65
N.11	6.10	0.012	4.54	10.08	0.014	4.72
N.12	6.08	0.012	2.30	10.07	0.015	4.86
N.13	6.08	0.009	3.75	10.08	0.008	5.10
N.14	6.09	0.014	4.21	10.05	0.003	4.48

Table 6. Diameter and roughness measurement for sample type M

	Gauge diameter			Head diameter		
Specimen ID	Mean [mm]	ST. Dev. [mm]	Roughness [µm]	Mean [mm]	ST. Dev. [mm]	Roughness [µm]
M.1	5.99	0.006	0.753	10.01	0.003	0.24
M.2	5.99	0.009	0.544	10.02	0.002	0.94
M.3	5.99	0.007	0.701	10.02	0.001	0.29
M.4	5.99	0.005	0.694	10.04	0.058	0.95
M.5	5.99	0.008	0.748	10.01	0.002	0.94
M.6	5.99	0.006	/	10.02	0.002	0.30
M.7	5.99	0.007	0.765	10.00	0.005	0.29
M.8	6.00	0.004	/	10.02	0.002	0.36
M.9	6.02	0.005	/	10.01	0.002	0.94
M.10	5.99	0.005	0.714	10.02	0.002	1.03

Tightening was done in such a way that specimen heads could not revolve in any chance inside chuck collets. It was also important to avoid overtightening, otherwise superposition of the chuck collet pressure and load may have occurred, which is likely to result in some irregular results. After specimen was mounted, radial misalignment of the gage section was checked. Total misalignment between spikes, was also checked for all samples during machining process. Testing was done under reversed bending load with stress ratio R=-1 and with the frequency of 60Hz. Fractographic and micrographic analysis have been done as well for some samples, after the end of the testing campaign to examine fracture initiation and propagation areas.

4. RESULTS

The results of the testing campaign are collected in Tables 7 to 9. The Tables provide data regarding specimen ID, applied loads, nominal stress value at the gage, observed life and comment regarding the trial outcome. In particular, "Run-out" indicates that the specimen survived testing at given load after 10^7 cycles, whereas "Yes" indicates that failure occurred. In this case the number of cucle to failure is also reported.

Table 7. Test results for sample type 1

Specimen ID	Load [N]	Stress [MPa]	Life [cycles]	Failure
1.1	211.9	699	2 277 295	Yes
1.2	201.6	665	3 374 203	Yes
1.3	180.5	596	6 090 458	Yes
1.4	158.9	524	-	Run-out
1.5	169.7	560	-	Run-out
1.6	169.7	560	-	Run-out
1.7	180.5	596	-	Run-out

Table 8. Test results for sample type H

Specimen ID	Load [N]	Stress [MPa]	Life [N]	Failure
H.1	211.8	699	85 768	Yes
H.2	184.9	610	120 572	Yes
H.3	157.4	520	127 820	Yes
H.4	103.0	340	-	Run-out
H.5	139.3	460	-	Run-out
H.6	148.6	490	-	Run-out
H.7	148.6	490	-	Run-out
H.8	157.4	520	-	Run-out
H.9	166.7	550	523 162	Yes
H.10	175.5	580	491 671	Yes
H.11	166.7	550	56 331	Yes
H.12	161.8	534	405 247	Yes

Table 8. Test results for sample type N

Specimen ID	Load [N]	Stress [MPa]	Life [N]	Failure
N.1	184.9	610	175 804	Yes
N.2	166.7	550	236 637	Yes
N.3	148.6	490	3 577 212	Yes
N.4	130.4	430	8 336 653	Yes
N.5	121.2	400	9 659 056	Yes
N.6	112.3	370	-	Run-out
N.7	121.2	400	-	Run-out
N.8	130.4	430	-	Run-out
N.9	139.3	460	8 069 582	Yes
N.10	130.4	430	-	Run-out
N.11	139.3	460	9 900 777	Yes
N.12	184.9	610	151 212	Yes
N.13	166.7	550	156 691	Yes
N.14	148.6	490	687 908	Yes

Table 9. Test results for sample type M

Specimen ID	Load [N]	Stress [MPa]	Life [N]	Failure
M.1	184.9	610	81 160	Yes
M.2	157.4	520	219 333	Yes

M.3	139.6	460	2 415 186	Yes
M.4	121.2	400	7 885 879	Yes
M.5	112.3	370	3 035 027	Yes
M.6	103.0	340	-	Run-out
M.7	112.3	370	7 879 073	Yes
M.8	103.0	340	-	Run-out
M.9	112.3	370	-	Run-out
M.10	121.2	400	5 662 050	Yes

Finally, each specimen was removed from the chuck collets and carefully examined for any irregularity.

5. DISCUSSION

The results of specimen testing presented in the previous Section were processed, to obtain the *S-N* curves in the finite life domain [35]. Curves trends with their upper and lower bounds for 90% confidence levels, obtained using linear regression method, are shown in Figures 6 to 9, using double logarithmic scale.

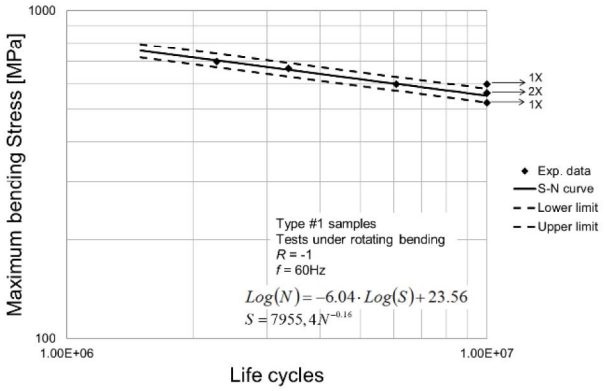

Figure 6. S-N Curve for sample type 1

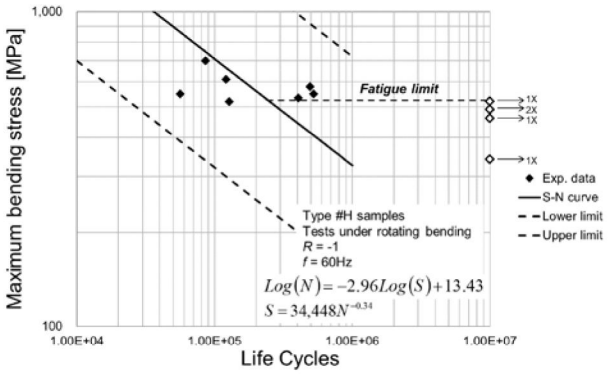

Figure 7. S-N Curve for type sample H

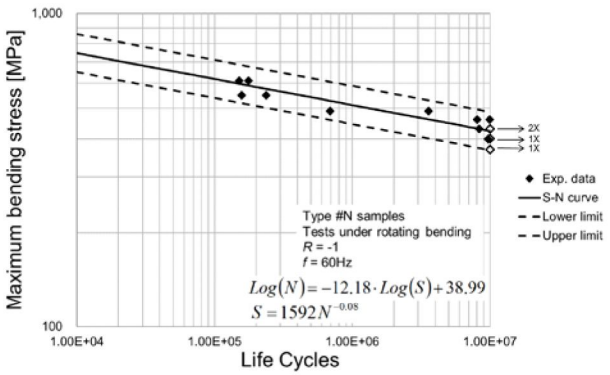

Figure 8. S-N Curve for sample type N

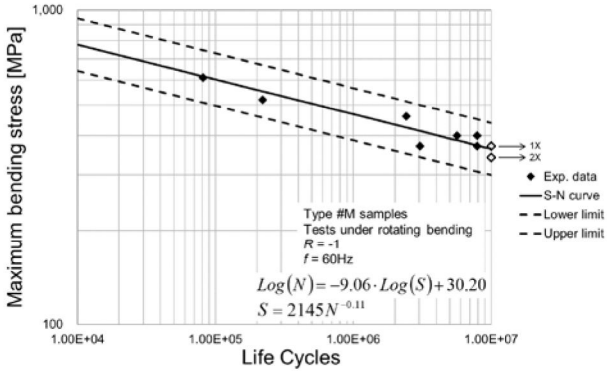

Figure 9. S-N Curve for sample type M

Details regarding specimen type, load ratio, testing frequency and the equation of the curve are also included in the same graphs. Run outs are marked with arrows on the graphs with indication of how many of them occurred at any load level. For all sample types, inclination angles between *S-N* curves and vertical axis were calculated. For sample type 1 the angle value it is 76°, for sample type H, it is 71°, for sample type N, 85° and for sample type M, 84°. Larger angle between the vertical axis and the *S-N* curve means that that those sample types are more sensitive to load increase. For those sample types with smaller angle value, the number of cycles to failure decreases less with load increase. Change in load leads to smaller change in cycle number. Sample types N and M exhibit a higher sensitivity to load increase than sample types 1 and H. A reason for this can be influence of age hardening, their hardness should be increased from 33-37 HRC to 50-56 HRC [31]. Sample type H exhibited greater scattering of the results than the other three sample types, which can be seen in Fig. 7. Specimens experienced failures at the same or close load levels with considerable differences in life cycle numbers, which also affected the unusual *S-N* curve inclination. As an effect of these outcomes, the confidence band for this curve is particularly wide (much wider than the others), which will probably require to run further tests at the next stages of this research.

Fatigue limit for every sample type was obtained using Dixon stair case method, based on the retrieved series of failure, and not-failure outcomes.

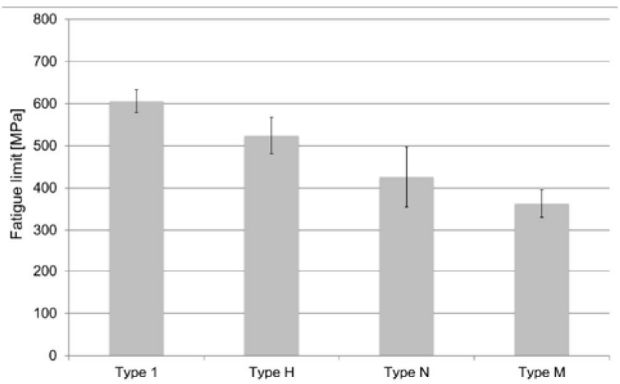

Figure 7. Fatigue limits with confidence bands

Fatigue limits for all sample types with their confidence band (95% confidence level) are presented in the bar graph in Fig. 7. The first two sample types underwent heat treatment, whereas the second two ones

were without heat treatment. The calculated value of *FL* for sample type 1 is 606MPa, for sample type H is 524MPa, for sample type N is 426MPa and for sample type M is 363MPa. These results indicate that heat treatment significantly enhances *FL*. *UTS* of MS1 maraging steel is 1100MPa in as the built condition, after hardening it is incremented up to 2050MPa, corresponding to almost 100% increase of *UTS*, following heat treatment [31]. Sample types 1 and H underwent hardening and their *FL* is respectively 29% and 25% of *UTS*. Sample types N and M were without hardening and their *FL* is indeed lower but respectively 39% and 33% of the corresponding *UTS* without heat treatment. These ratios are much lower than the commonly accepted ratios of *FL* over *UTS* of 50% for machined samples, but are in agreement with some literature research, when considering as built parts [38-39]. This is not surprising, due to the layered characteristic of specimens. Sample type N had greater *FL,* than machined sample type M. Both samples were without any heat treatment. First, it must be observed that the difference between type N and type M fatigue strengths is quite small: a statistical test, based on the Analysis of Variance and on the Fisher-test, indicated that these differences are not significant at the 5% significance level. Anyway, some possible reasons for unmachined samples having a better performance than machined ones is provided in the following. Sample types N had greater surface roughness than types M. This is possible outcome of shot peening which is known to have positive effect on *FL* [40].

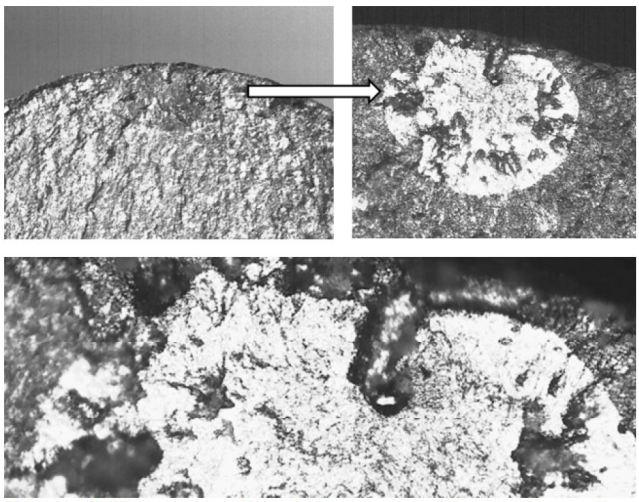

Figure 8. Pore in crack initiation zone, close to the surface for H.5 specimen

The surfaces of the sample types N were hardened by shot peening plastic deformation, and all micro pores were closed as a result of this process, conversely for sample type M, this effect is shadowed because of the machining. Machining also took possible irregularities and porosities inside material to surface, which are possible sources of premature crack initiations [27].

The previous statement can be confirmed by the many porosities and voids revealed during fractographic and micrographic analysis. During fractographic analysis of break surface of both sides of the broken sample, it was found that crack initiation and nucleation starts at one point on the surface or just beneath it, as shown in Fig. 8. Some amount of voids and inclusions were noticed on fractured surface of all samples. It is indeed possible that voids or inclusions were responsible for crack initiation: most cracks seem to start from such defects. On all the samples, only one crack initiation point was noticed. There have been some doubts for as built samples, due to surface roughness influence (notch effect).

Fracture surface of as built samples without heat treatment showed coarse-grained structure.

Some specimens were cut, embedded into phenolic resin, and polished for micrographic analysis Fig.9.

Figure 9. Specimen preparation for micrography

Specimen surface was etched with combination of 150cc of water (H_2O), 50cc of Chloridric Acid (HCl), 25cc of Nitric Acid (HNO_3) and 1g of Calcium Chloride. Etching was done at room temperature for 70 seconds. It must be pointed out that laser scanning traces were visible both in longitudinal and in transverse sections, regardless of heat treatment execution.

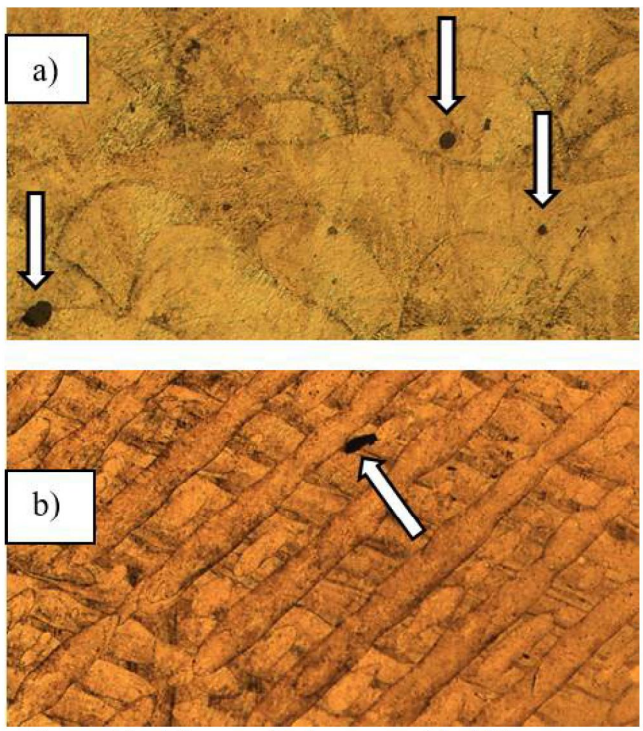

Figure 10. a) Longitudinal section of the N.2 specimen without heat treatment

b) Build plane section (normal to specimen axis)

Some inclusions were noticed and marked with arrows in Fig.10. Scanning pattern in build plane section Fig.10 b), shows some scanning traces underneath with rotation angles corresponding to the aforementioned angle of 67°. Specimens without heat treatment had more pronounced scanning traces that those that had undergone the heat treatment by age hardening (see Fig 11). This outcome indicates that heat treatment had some effect on

fusion of the laser traces but was not effective at completing deleting these traces. For all the four sample types a comparable amount of inclusion was observed. Heat treatment had no effect on the presence of porosities in material.

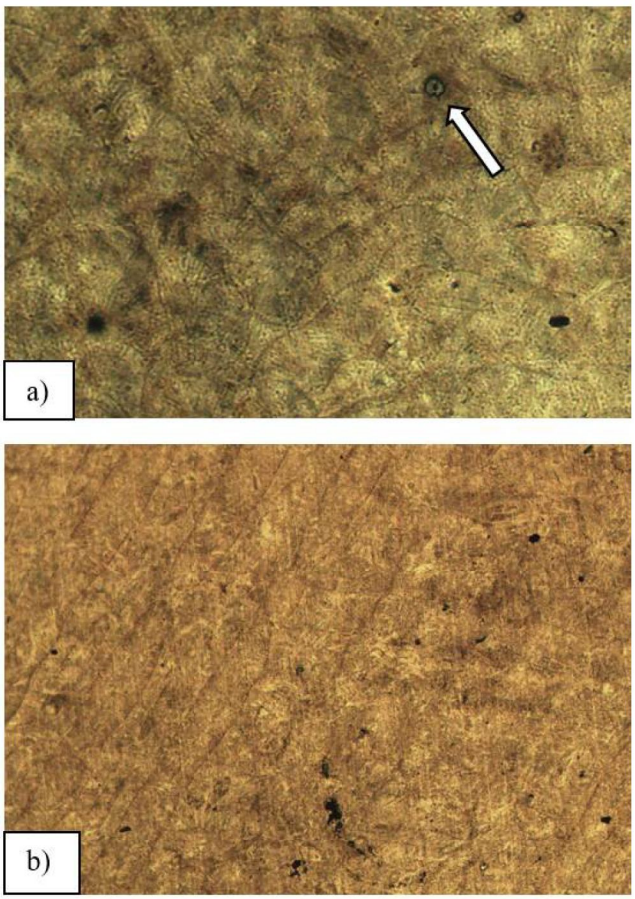

Figure 11. a) Longitudinal section of the specimen with heat treatment

b) Build plane section (normal to specimen axis)

6. CONCLUSION

This paper aims at a study on machining and heat treatment effects on fatigue limit and fatigue strength of Maraging Steel specimens manufactured by DMLS EOSINT M280 machinc. Four samplc scts wcrc considered, all with vertical stacking direction during building. No deformation of the specimens as a result of residual stresses was observed. All the sets were shot peened as part of cleaning process. Two sets underwent machining procedure for 0.5mm allowance and two were left in the as built surface state. One machined and one as built set were heat treated by age hardening in oven. All sample sets were then tested under four point bending tested with R=-1 load ratio at the frequency of 60Hz. All the experimental results were processed for the determination of S-N curves in the finite life domain and fatigue limits. The heat treated samples exhibited steeper S-N curve than the samples without heat treatment. Moreover, heat treated samples without machining exhibited a great result scattering that can be attributed to notch effect deriving from surface roughness. Anyway, this outcome will need further testing and investigations at the next stages of the research. Heat treated sample types had greater fatigue limits than samples without heat treatment. Fatigue strength to ultimate tensile strength ratio for unmachined heat treated samples was around 25%, which is consistent with other research but lower than the corresponding ratios for the other two sample sets. In fact, when running comparative analysis, it must be noticed that the ultimate tensile strength for samples without heat treatment is almost one-half of the value for heat treated ones.

Machined samples without heat treatment had lowest ultimate tensile strength. A possible reason is that, following machining, pores, inclusions and micro cracks were brought to the surface and became source of micro stress concentration, thus inducing crack initiation and detrimentally affecting fatigue limit. In addition, the hardened surface obtained by plastic deformation (and the related compressive residual stress state) via shot peening was also taken away, which is not the case for as built sample without heat treatment, resulting in a greater fatigue limit.

in the future it could be possible to expand research with shot peening effect on machined samples after machining. In this way all the pores and microcraks brought to surface would be closed, the surface would be hardened by plastic deformation and a potentially beneficial compressive residual stress state could be induced.

ACKNOWLEDGEMENTS

This paper represents a part of research performed within the project "Advanced design rules for optimal dynamic properties of additive manufacturing products - A_MADAM", which received funding from the European Union's Horizon 2020 research and innovation programme under the Marie Skłodowska-Curie grant agreement No.734455.

Two of the authors (S. Ćirić-Kostić and A. Vranić) wish also to acknowledge the support of Ministry of Education, Science and Technology Development of Republic of Serbia through grants No.TR35006 and No.TR37020.

REFERENCES

[1] Bourell, D.L., Beaman, J.J., Leu, M.C. and Rosen, D.W., 2009. A brief history of additive manufacturing and the 2009 roadmap for additive manufacturing: looking back and looking ahead. Proceedings of RapidTech, pp.24-25.

[2] Aliakbari, M. "Additive manufacturing: State-of-the-art, capabilities, and sample applications with cost analysis." (2012).

[3] Pandey, P.M., 2010. Rapid prototyping technologies, applications and part deposition planning. Retrieved October, 15.

[4] Herderick, E. "Additive manufacturing of metals: A review." Materials Science & Technology (2011): 1413-1425.

[5] Shellabear, M., and O. Nyrhilä. "DMLS-Development history and state of the art." Laser Assisted Netshape Engineering 4, Proceedings of the 4th LANE (2004): pp. 21-24.

[6] Campanelli, S.L., Contuzzi, N., Angelastro, A. and Ludovico, A.D., 2010. Capabilities and performances of the selective laser melting process. In New Trends in Technologies: Devices, Computer, Communication and Industrial Systems. InTech.

[7] Naiju, C. D., M. Adithan, and P. Radhakrishnan. "An Investigation of Process Variables Influencing Fatigue Properties of Components Produced by Direct Metal Laser Sintering." KMUTNB: International Journal of Applied Science and Technology 4.1 (2011): pp. 63-69.

[8] Parthasarathy, J., Starly, B. and Raman, S., 2011. A design for the additive manufacture of functionally graded porous structures with tailored mechanical properties for biomedical applications. Journal of Manufacturing Processes, 13(2), pp.160-170.

[9] Jardini, A. L., M. A. Larosa, M. F. Macedo, L. F. Bernardes, C. S. Lambert, C. A. C. Zavaglia, R. Maciel Filho, D. R. Calderoni, E. Ghizoni, and P. Kharmandayan. "Improvement in Cranioplasty: Advanced Prosthesis Biomanufacturing." Procedia CIRP 49 (2016): pp. 203-208.

[10] Jardini, A.L., Larosa, M.A., Maciel Filho, R., de Carvalho Zavaglia, C.A., Bernardes, L.F., Lambert, C.S., Calderoni, D.R. and Kharmandayan, P., 2014. Cranial reconstruction: 3D biomodel and custom-built implant created using additive manufacturing. Journal of Cranio-Maxillofacial Surgery, 42(8), pp.1877-1884.

[11] Bertol, L.S., Júnior, W.K., da Silva, F.P. and Aumund-Kopp, C., 2010. Medical design: direct metal laser sintering of Ti–6Al–4V. Materials & Design, 31(8), pp.3982-3988.

[12] https://www.eos.info/material-m

[13] Brookes, K.J., 2016. Maraging steel for additive manufacturing–Philipp Stoll's paper at DDMC 2016. Metal Powder Report, 3(71), pp.149-152.

[14] Yasa, E., Kempen, K., Kruth, J.P., Thijs, L. and Van Humbeeck, J., 2010, August. Microstructure and mechanical properties of maraging steel 300 after selective laser melting. In Solid Freeform Fabrication Symposium Proceedings (pp. 383-396).

[15] Kempen, K., Yasa, E., Thijs, L., Kruth, J.P. and Van Humbeeck, J., 2011. Microstructure and mechanical properties of Selective Laser Melted 18Ni-300 steel. Physics Procedia, 12, pp.255-263.

[16] Casalino, G., Campanelli, S.L., Contuzzi, N. and Ludovico, A.D., 2015. Experimental investigation and statistical optimisation of the selective laser melting process of a maraging steel. Optics & Laser Technology, 65, pp.151-158.

[17] https://www.eos.info/industries_markets/aerospace/engines

[18] 18. Croccolo, D., De Agostinis, M., Fini, S., Olmi, G., Vranic, A., Ciric-Kostic, S.: "Influence of the build orientation on the fatigue strength of EOS maraging steel produced by additive metal machine", Fatigue and Fracture of Engineering Materials and Structures 39 (5) (2016), pp. 637-647

[19] Casati, R., Lemke, J.N., Tuissi, A. and Vedani, M., 2016. Aging Behaviour and Mechanical Performance of 18-Ni 300 Steel Processed by Selective Laser Melting. Metals, 6(9), p.218.

[20] Gibson, I. and Shi, D., 1997. Material properties and fabrication parameters in selective laser sintering process. Rapid Prototyping Journal, 3(4), pp.129-136.

[21] Baufeld, B., Van der Biest, O. and Gault, R., 2010. Additive manufacturing of Ti–6Al–4V components by shaped metal deposition: microstructure and mechanical properties. Materials & Design, 31, pp. S106-S111.

[22] Edwards, P. and Ramulu, M., 2014. Fatigue performance evaluation of selective laser melted Ti–6Al–4V. Materials Science and Engineering: A, 598, pp.327-337.

[23] Bača, A., Konečná, R., Nicoletto, G. and Kunz, L., 2016. Influence of build direction on the fatigue behaviour of Ti6Al4V alloy produced by direct metal laser sintering. Materials Today: Proceedings, 3(4), pp.921-924.

[24] de Vree, W.K., 2016. On the influence of build orientation on the mechanical properties of direct metal laser sintered (DMLS) Ti-6Al-4V flexures.

[25] Konečná, R., Kunz, L., Bača, A. and Nicoletto, G., 2016. Long fatigue crack growth in Ti6Al4V produced by direct metal laser sintering. Procedia Engineering, 160, pp.69-76.

[26] Smith, D.H., Bicknell, J., Jorgensen, L., Patterson, B.M., Cordes, N.L., Tsukrov, I. and Knezevic, M., 2016. Microstructure and mechanical behavior of direct metal laser sintered Inconel alloy 718. Materials Characterization, 113, pp.1-9.

[27] Brandl, E., Heckenberger, U., Holzinger, V. and Buchbinder, D., 2012. Additive manufactured AlSi10Mg samples using Selective Laser Melting (SLM): Microstructure, high cycle fatigue, and fracture behavior. Materials & Design, 34, pp.159-169.

[28] Lewandowski, J.J. and Seifi, M., 2016. Metal additive manufacturing: a review of mechanical properties. Annual Review of Materials Research, 46, pp.151-186.

[29] International Organization for Standardization ISO 1143:2010 (E) (2010) Metallic Materials – Rotating Bar Bending Fatigue Testing, International Organization for Standardization (ISO), Geneva, Switzerland.

[30] https://www.eos.info/systems_solutions/metal/systems_equipment/eosint_m280

[31] https://www.eos.info/material_m/werkstoffe/download/EOS_MaragingSteel_MS1.pdf

[32] Sanz, C. and Navas, V.G., 2013. Structural integrity of direct metal laser sintered parts subjected to thermal and finishing treatments. Journal of Materials Processing Technology, 213(12), pp.2126-2136.

[33] Aboulkhair, N.T., Maskery, I., Tuck, C., Ashcroft, I. and Everitt, N.M., 2016. Improving the fatigue behaviour of a selectively laser melted aluminium alloy: Influence of heat treatment and surface quality. Materials & Design, 104, pp.174-182.

[34] Dixon, W.J. and Massey, F.J., 1969. Introduction to statistical analysis (Vol. 344). New York: McGraw-Hill.

[35] International Organization for Standardization ISO 12107:2003, “Metallic Materials – Fatigue Testing – Statistical Planning and Analysis of Data”, International Organization for Standardization (ISO), Geneva, Switzerland, (2003)

[36] Bunker, R. S. Innovative gas turbine cooling techniques. WIT Press, Southampton, UK, 2008.

[37] Kasperovich, G. and Hausmann, J., 2015. Improvement of fatigue resistance and ductility of TiAl6V4 processed by selective laser melting. Journal of Materials Processing Technology, 220, pp.202-214.

[38] Stoffregen, H.A., Butterweck, K. and Abele, E., 2014. Fatigue analysis in selective laser melting: review and investigation of thin-walled actuator housings. In 25th Solid Freeform Fabrication Symp.

[39] Niemann, G., Winter, H. and Hohn, B. R. (2005) Maschinenelemente, Springer-Verlag: Berlin Germany.

[40] Olmi, G. and Freddi, A., 2013. A new method for modelling the support effect under rotating bending fatigue: application to Ti-6Al-4V alloy, with and without shot peening. Fatigue & Fracture of Engineering Materials & Structures, 36(10), pp.981-993.